CHEMISTRY
A EUROPEAN JOURNAL

DOI: 10.1002/chem.200903259

Sonication-Assisted Fabrication and Post-Synthetic Modifications of Graphene-Like Materials

Giancarlo Cravotto*[a] and Pedro Cintas*[b]

Dedicated to Professor Josep M. Ribó on the occasion of his 70th birthday

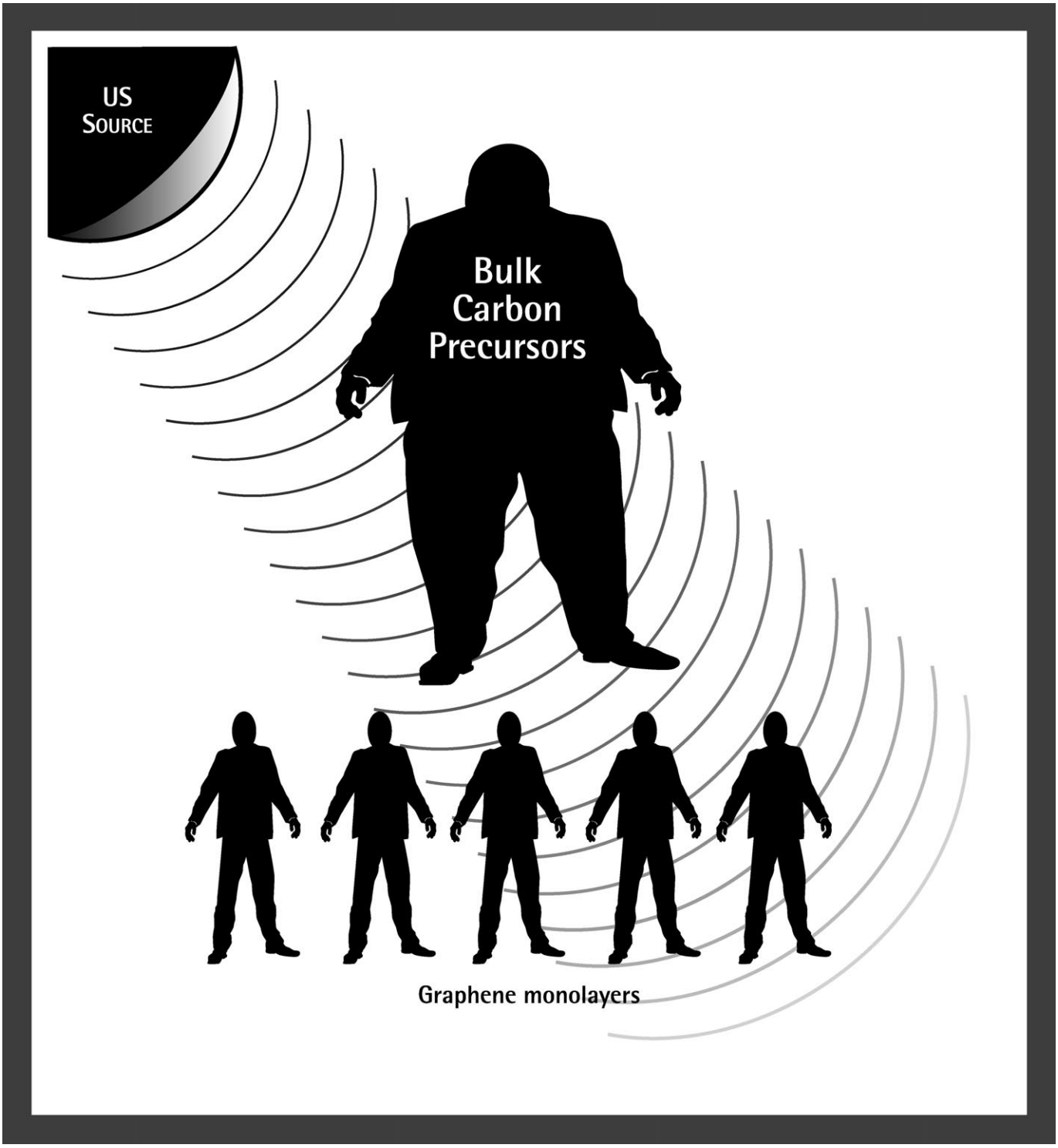

Abstract: Chemistry of and with graphene constitutes a rapidly evolving field that holds much promise for the generation of advanced materials with salient, and often unique, properties and potential applications in different fields. However, reliable, mild, and scalable methods to produce this layered carbonaceous material represent an important bottleneck and are critical for progress in this research area to continue. In this context, the use of ultrasound has become a routine and indispensable step in numerous synthetic protocols, even though most researchers usually overlook the science behind it. This minireview provides some fundamentals on the interaction of sound waves with matter and equally illustrates how sonication assists further synthetic decorations under benign conditions.

Keywords: carbon · graphene · graphite · nanotechnology · synthetic methods · ultrasound

Graphene: Insights into Concepts

Like fullerenes and carbon nanotubes in past decades, excitement and spectacular interest in graphene have become a matter for chemical sociology. This discovery is of course mesmerizing and beyond hype, although it is still obscure to the everyday consumer. Graphene denotes a two-dimensional (2D) material consisting of monolayer, sp^2-hybridized, carbon atoms arranged in six-membered rings. It is ideally flat, though thermal fluctuation causes temporary ripples. Graphene materials, which include not only single-layer structures, but also arrays of a few monolayers, exhibit unique molecular and quantum properties that make them promising candidates for a wide variety of technological applications.[1] Although the term graphene has been coined in recent years, the search for a perfect monolayer of a 2D crystal structure is not conceptually new. In fact, the term *monolayer graphite* has been employed for more than four decades to denote an active research area that culminated ultimately in what is now referred to as graphene.[2] In the late 1990s, it was evident that micromechanical exfoliation of highly pyrolytic graphite (HOPG) resulted in very thin platelets, which could presumably include single carbon layers as well.[3] However, on the basis of older theoretical studies, it was believed that 2D crystals would be thermodynamically unstable at moderate temperatures. This conjecture proved to be wrong when Geim and associates isolated in 2004 the first samples of single carbon layers by mechanical exfoliation of 3D graphite. The peeling method is extraordinarily simple and consists essentially in removing successive layers from a graphite flake by rubbing against another surface, such as a common cellophane tape. This strategy usually results in flakes of multiple layers, though delaminated samples that are only one layer thick can be detected.[4] This manual procedure requires both practice and patience to get reproducible results; monolayers, invisible to the naked eye, can be screened by microscopy techniques.[5]

The above-mentioned mechanical cleavage is not suitable for large-scale (i.e., gram or multigram) synthesis. Improved methods can be classed into two main strategies:[1c] 1) transformation involving graphite as precursor or an all-carbon material, and 2) exfoliation of an oxygen-containing laminar structure (usually graphite oxide, GO) followed by reduction. Method 1 can be accomplished by different routes (some available to specialized laboratories only) such as H-arc discharge, chemical vapor deposition (CVD) on surfaces, epitaxial growth from the high-temperature reduction of SiC under ultrahigh vacuum, or dispersion in appropriate solvents. Method 2 has become particularly attractive as GO can be readily obtained and is interesting in its own right for materials science applications. Reduction of GO leads to chemically modified graphene, in which oxygen functionalities (both OH and epoxy groups; vide infra) are replaced by other functional groups. A substrate-free, gas-phase, graphene synthesis is also capable of producing a material similar to that obtained through exfoliation.[6] In addition, a series of bottom-up self-assembly approaches have been explored to construct graphene-like structures. Here, an organic precursor serves as a template-directing agent and source of carbon atoms.[7]

It is worth noting that numerous methods to produce graphene and graphene-derived compounds involve the use of sonication (more precisely *ultrasonication*) as an important, often key, experimental step. This unique and innocuous irradiation appears to be vastly superior to other mechanical energies and contributes to create a laminated material and/or favor formation of stable colloidal dispersions, even with deoxygenated sheets, which, due to the lack of hydrophilicity, are prone to aggregation.

What is actually behind sonication and how can its role be rationalized? The effects of ultrasound on materials are in principle well established and two major contributions arise from cavitation (growth and collapse of micrometer-sized bubbles) and shear forces. An outstanding and comprehensive review by Skrabalack has recently documented the synthesis of different carbonaceous materials aided by both ultrasonic spray pyrolysis and high-intensity ultrasound.[8]

[a] Prof. Dr. G. Cravotto
Dipartimento di Scienza e Tecnologia del Farmaco
Università di Torino, Via Giuria 9, 10125 Torino (Italy)
Fax: (+39) 011-670-7687
E-mail: giancarlo.cravotto@unito.it

[b] Prof. Dr. P. Cintas
Departamento de Química Orgánica e Inorgánica
Facultad de Ciencias-UEX, E-06071 Badajoz (Spain)
Fax: (+34) 924-271-149
E-mail: pecintas@unex.es

Here we report the conceptual basis of the interaction of sound waves with ordered matter. Like other physical fields, structure–property relationships can be mathematically described and are influenced by anisotropy and symmetry considerations. A rigorous analysis requires both tensors and matrices, though we will not go beyond a descriptive and, it is hoped, understandable treatment. Further illustrations on the effects of sonication on graphitic materials en route to graphenes and related structures will be discussed.

Sound Waves and Mechanical Forces

Acoustic waves consist of alternating regions of compression and rarefaction. This radiation, unlike electromagnetic waves, lacks quantum nature and the commonly used ultrasonic frequencies refer to the range beyond human hearing (18–20 kHz). An acoustic wave can be described by two vectors: a wave normal (N) and a particle motion vector (U) (Figure 1). In solids, both longitudinal waves (in which U is

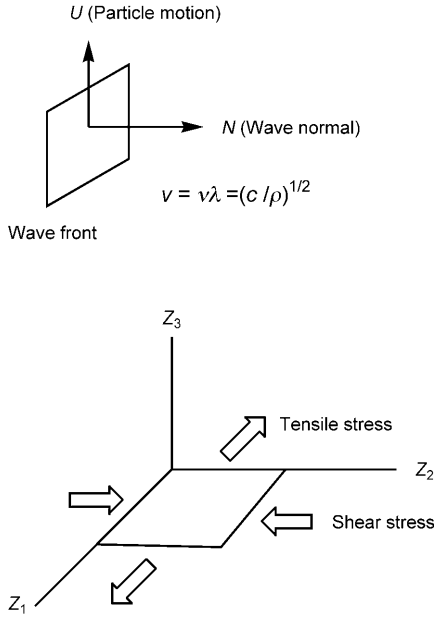

Figure 1. Schematic representation of acoustic waves and stress gradients for tensile and shear forces.

parallel to N) and shear waves (particle displacement lies in the perpendicular direction) are observed, while only longitudinal waves are present in liquids. Acoustic wave velocities (v) are controlled by elastic constants (c) and density (ρ). Sound is transmitted faster in, for instance, light metals, which possess stronger and shorter bonds than heavy atoms.

In linear acoustics, the Christoffel equation relates the ultrasonic wave velocities, wave normals, polarization directions, and elastic constants, and can be obtained from the plane wave solution to the equation of motion applied to a differential volume element [Eq. (1)],[9] in which U_k and N_j are the direction cosines of the particle motion and wave normal, respectively.

$$\rho v^2 U_i = c_{ijkl} N_j U_k N_l \quad (1)$$

For any given wave normal, there are always three solutions to the Christoffel equation, which are markedly dependent on the symmetry properties in agreement with the general Curie and Newmann principles. If the wave normal has a certain symmetry, then the vibration directions of the three associated acoustic waves must conform to that symmetry.[9] In solids without symmetry restrictions, the three waves will travel with different velocities and different vibration directions that are perpendicular to one another. For a hexagonal lattice, there are three acoustic waves traveling along the [100] axis: a longitudinal wave polarized parallel to [100], a shear wave polarized to [120], and another wave polarized parallel to [001]. The longitudinal wave propagates faster because the elastic constant c_{11} is usually larger than the other coefficients.

Graphite is not only a layered material, but also anisotropic. The latter arises from a particular structure in which strong, covalent, sp^2 bonds forming the σ network coexist with bands of filled π orbitals (the valence band) and empty π* orbitals (the conduction band). Since there is no bonding in the c axis, out-of-plane interactions are weak and as a result graphite's out-of-plane electrical and thermal conduc-

Giancarlo Cravotto, a graduate in Pharmacy and in Pharmaceutical Chemistry and Technology, after a three-year experience in the pharmaceutical industry, became a researcher in organic chemistry at the University of Torino. He is currently Full Professor of Organic Chemistry and in July 2007 he was elected Director of the Dipartimento di Scienza e Tecnologia del Farmaco. His research activity has been centered on the synthesis of natural products and fine chemicals. These studies have paved the road to new synthetic procedures under non-conventional conditions (ultrasound- and microwave-assisted reactions). He has authored about 150 peer-reviewed papers, 4 book chapters and 15 patents.

Pedro Cintas has taught at the University of Extremadura (Spain) since 1990 after a postdoctoral stay in Geneva (Switzerland) working under Wolfgang Oppolzer on asymmetric synthesis of N-alkylated amino acids. Trained in carbohydrate chemistry (Ph.D in 1987) and stereochemistry, he later developed a further interest in non-conventional methods of physical activation. A member of the advisory board of Ultrasonics Sonochemistry and the scientific committee of the European Society of Sonochemistry, he chaired the 9th international meeting of this society in 2004.

tivities are considerably smaller than the in-plane components. In an isotropic material the energy flow (of an elastic wave) is parallel to the wave normal; however, in anisotropic crystals the two vectors are generally oriented differently. In other words, acoustic anisotropy occurs in crystals possessing anisotropic bonding. Graphite having a hexagonal crystal structure possesses an extreme elastic anisotropy with easy cleavage between the layers. The elastic stiffness coefficient c_{11} is much larger than c_{33}, and c_{66} is larger than c_{44}. This situation, though less pronounced, is also found in hexagonal close-packed metals, which have slightly longer bonds in the [001] plane. There are some exceptions; for example, Zn, which has shorter Zn–Zn bonds in the [001] plane and the elastic coefficients $c_{11}=c_{22}$ are greater than c_{33}. As a consequence the structure is stiffer in the Z_1 and Z_2 plane directions. Thus longitudinal acoustic waves along Z_3 (the sixfold symmetry axis) are slower than in the perpendicular directions (Figure 1). A similar pattern occurs in layered metal structures (e.g., trigonal bismuth) with easy cleavage and stiffest in the Z_1–Z_2 plane.[10]

While an anisotropic material undergoes predicted deformations and stress in an acoustic field, cavitation will exert the major contribution to mechanical and chemical effects assuming ultrasonication of sufficient intensity. Cavitation is a nonlinear phenomenon and departures from the Christoffel equation are not easy to model. From a qualitative viewpoint, cavitation concentrates low-density, elastic (sound) wave energy into higher densities by rapid bubble collapse. The resulting extreme local conditions induce profound changes at the solid–liquid interface. Collapse on the surface itself will cause direct damage by the shock waves produced, whereas collapse in the liquid close to a surface causes a microjet of solvent to hit the solid with great force.[11,12] This pitting effect is responsible for the well-known cleaning effect of ultrasound waves, thereby enhancing surface reactivity and promoting the encounter of reactive species. The mechanical energy is also sufficient to remove top layers after disrupting weak molecular interactions leading to delamination and dispersion.

Numerical estimations of the forces acting on particles near a collapsing bubble are, however, less accurate. Large strain rates ($d\varepsilon/dt$ of up $10^9\,s^{-1}$) are predicted for the radial elongation around a cavitation bubble, which should directly influence the stress experienced by particles in a sonicated fluid. Friction arising from the velocity difference between a solid particle and the surrounding liquid will cause viscous forces at the interfaces capable of cutting the particles. A series of models have been proposed for rodlike molecules such as carbon nanotubes (CNTs), for which the frictional force approaches $\mu(d\varepsilon/dt)L^2$, in which μ is the fluid viscosity and L the length of the nanotube.[13,14] Although this assumption could not be extrapolated to other carbon forms, it would provide approximate estimations of the kinetics of the phenomenon and the average length obtained after sonication. A major drawback is the fact that the flow may not be laminar under these conditions and turbulence also affects the scission of large molecules.[15] This complex issue lies beyond the scope of this article, although we shall briefly see it later as CNTs can be precursors of graphene and vice versa.

Graphite Exfoliation

Although the properties of graphene are quite different from those of graphite and other carbon allotropes, graphene could be viewed as a quintessential graphite layer. Graphene was in fact considered a virtual molecule for a long time. Carbon materials can be transformed into carbon layers under sonication. However, the method as a whole is rather unpractical to produce high concentrations of single layers. Carbon nanoparticles and nanotubes, for instance, undergo mechanical damage by ultrasound in organic solvents. Nanoparticles are even more sensitive and prolonged sonication leads to amorphous carbon. Sonication also causes deformation and bending of nanotubes. Raman and ESR spectroscopy reveal an increase of the band at $1286\,cm^{-1}$ attributed to in-plane vibrations of graphene layers; this method can be used to monitor the extent of damage induced by ultrasound.[16]

Ultrasonic treatment of HOPG in water also produces carbon nanospheres composed of disordered graphene sheets with thickness ranging from 10 nm to 200 nm (equivalent to ≈30–600 layers), still far from an ideal single layer. Clearly ultrasound breaks the graphitic basal structure and results in carbon fragments of variable size. Irradiation time controls nucleation and growth, and prolonged sonication favors condensation by a rolling snow-ball mechanism.[17]

Even inexpensive carbon black can be used to fabricate carbon nanosheets upon ultrasonic irradiation (60 kHz, 90 W, RT, N_2 atmosphere).[18] High-resolution TEM images reveal formation of sheets with an average interlayer spacing of about 0.34 nm (3.4 Å), which is typically found in the hexagonal lattice of graphite. This suggests that such sheets are composed of graphite layers. AFM images estimated the thickness of each sheet in a few nanometers (from 1.23 to 2.69 nm; Figure 2). Unfortunately, such sheet-like materials exhibit numerous distortions. Carbon sheets moving at high speed under the action of turbulent flow and shock waves fragment into carbon atom networks, which subsequently self-assemble to a 2D hexagonal cluster and then to a graphitic sheet.[18]

A suitable starting point to produce graphene would be graphite intercalation compounds (GICs); these are layered materials in which the interlayer spacing can increase considerably relative to native graphite (from 0.34 nm to more than 1 nm). GICs are also powerful reducing agents, but their preparation usually requires high temperatures (150–200 °C) for several hours. Ultrasound itself accelerates and facilitates the preparation of GICs, such as KC_8, without requiring external heating.[19] Intercalations of bulky atoms like metal complexes are likewise improved by sonication.[20] Metal intercalation changes graphite coloration, as a result of the delocalization of metal electrons into the graphite

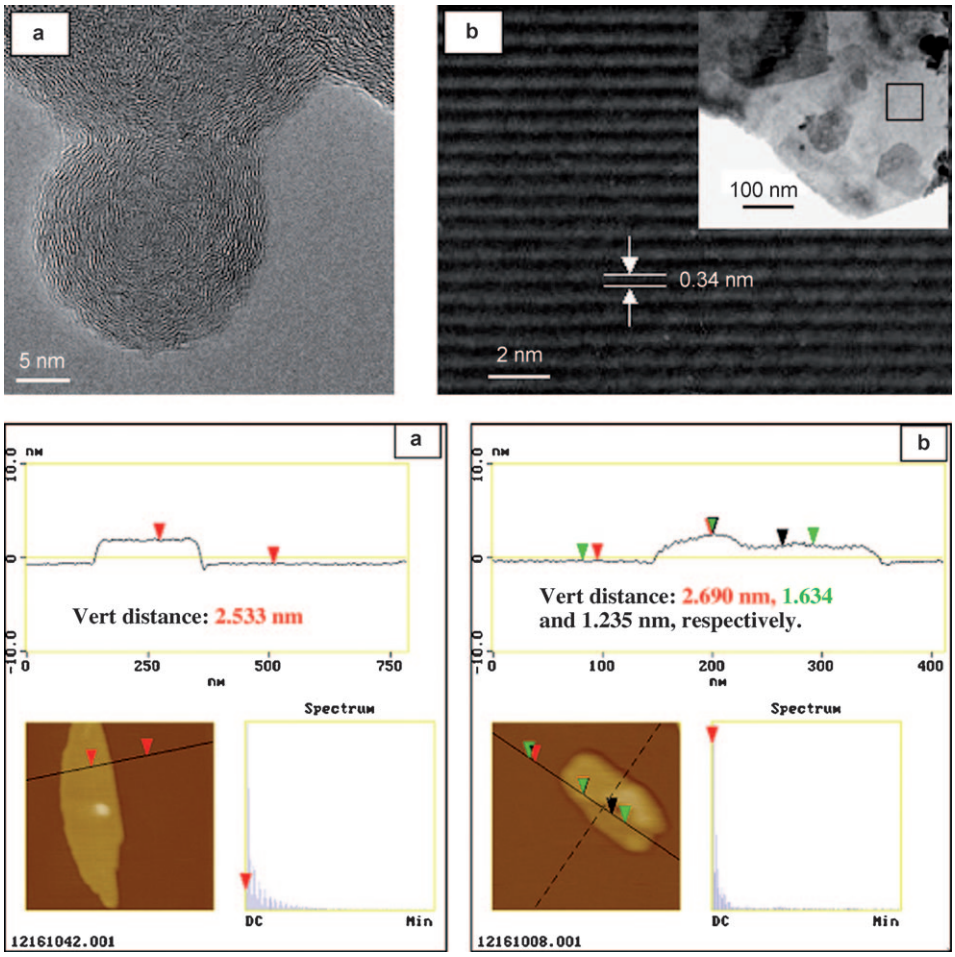

Figure 2. HR-TEM images of a) carbon black and b) sheet-like material obtained by sonication. AFM images (below) of the sheet structure. Reproduced with permission from reference [18]. Copyright 2007 by Elsevier Ltd.

conduction band, and significantly reduces the weak forces between adjacent sheets. Bearing this in mind, Kaner and associates reasonably thought of using KC_8 as a precursor for graphene layers by further treatment with alcohols under sonication.[21] Exfoliation does actually occur, although typical pillars of around 30 layers thick tend to scroll under sonication as well (Figure 3).

Dai and co-workers further exploited graphite intercalation to produce graphene nanoribbons down to 10 nm width.[22] The team used graphite flakes, which were expanded by intercalation with an oxidizing mixture of sulfuric and nitric acid (oxidation occurring likely at edges and defect sites). A rapid heating (60 s) to 1000 °C in a H_2/Ar mixture causes disruption of the intercalant and exfoliates graphite into pillars of a few layered graphene sheets. Sonication in CH_2Cl_2 for 30 min in the presence of a copolymer, poly(*m*-phenylenevinylene-2,5-dioctoxy-*p*-phenylenevinylene) (PmPV), led to a stable dispersion of graphene sheets. Although the PmPV copolymers absorb onto single-walled carbon nanotubes (SWCNTs) through π-stacking, they noncovalently decorated graphene sheets during sonication to yield a black suspension. The latter could not be obtained in the absence of

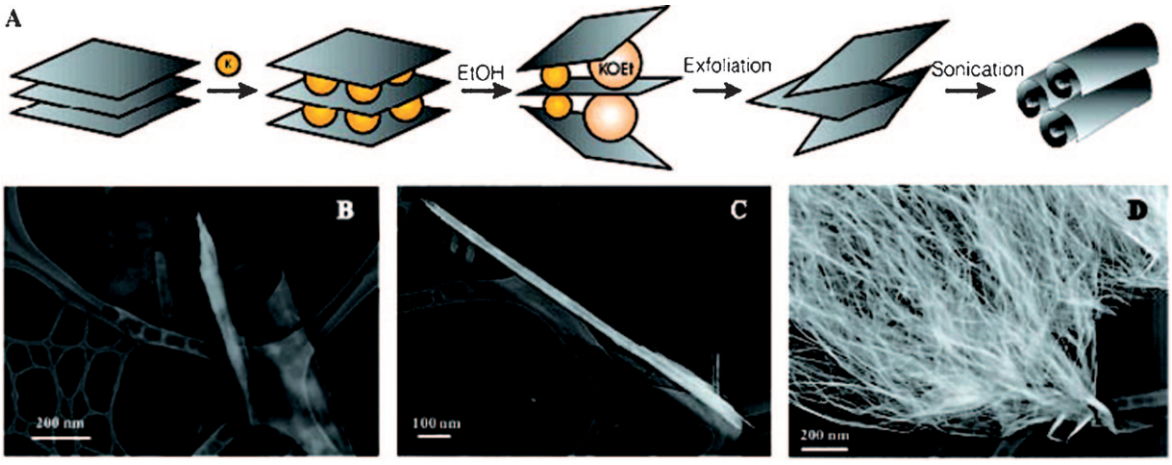

Figure 3. A) Schematic representation of sonication-assisted exfoliation and assembly from graphite intercalation compounds; TEM images of graphite sheets in B) scrolling, C) isolated nanoscroll, and D) bulk scrolled material. Reproduced with permission from reference [21a]. Copyright 2003 by the American Association for the Advancement of Science.

PmPV. The authors point to sonication as being responsible for the mechanically induced breaking of the graphene sheets into smaller fragments. Such a mechanochemistry assisted by bubble collapse produces various graphene morphologies, including regularly shaped nanoribbons (Figure 4).

The ability of sonication in producing narrow ribbons is remarkable; however, irradiation times should be controlled to produce optimal yields. As one might have anticipated, prolonged sonication is detrimental and leads to small carbonaceous particles. It is also important to mention that, unlike SWCNTs, the nanometer-sized graphene ribbons are semiconductors and enable the fabrication of field-effect transistor devices with high on–off ratios at room temperature. This research group has also obtained graphene nanoribbons by plasma etching of multiwalled carbon nanotubes (MWCNTs), which were previously dispersed by a brief sonication and then deposited onto a polymer film.[23]

The above-mentioned oxidative intercalation of graphite resembles a recent and quite simple protocol, without sonication nevertheless, developed by Tour and associates, for unzipping MWCNTs with H_2SO_4 and $KMnO_4$. This chemical treatment followed by moderate heating gives rise to a nearly quantitative yield of graphene nanoribbons up to 4 μm long, widths of 100–500 nm, and variable thicknesses (1–30 graphene layers).[24] From a mechanistic viewpoint, the unzipping reaction most likely involves carbon–carbon double-bond oxidation in the nanotubes. However an intercalation-like process of the acid between the CNT cylinders should not be excluded.

It appears that MWCNTs are readily broken in an ultrasonic field. In the presence of a standard polymer, such as polyvinylpyrrolidone (PVP), which can also be decomposed into radicals by ultrasonic irradiation, polymer-grafted nanotubes are obtained. This material has a greater stability than the parent MWCNTs and can be dispersed in polar solvents.[25]

Graphene sheets have likewise been fabricated from expandable graphite (generated by thermal treatment of commercial graphite as above), followed by intercalation with oleum (H_2SO_4 containing 20% SO_3) and subsequent reaction with tetrabutylammonium hydroxide in DMF.[26] Overall the procedure contributes to increase the distance between graphite layers still further. This highly intercalated graphite is sonicated for 60 min in a solution of a PEGylated phospholipid, 1,2-distearoyl-glycero-3-phosphoethanolamine-*N*-[methoxy-(PEG)-5000] (DSPE-mPEG), in DMF leading to a homogeneous suspension of graphene sheets coated with lipid molecules. AFM images reveal average sizes of 250 nm and heights of approximately 1 nm.

Geim and co-workers used ultrasonic cleavage as alternative route to the manual and time-consuming scotch-tape technique. Thus, graphite flakes can easily be obtained by sonicating graphite crystals in DMF for over 3 h. The resulting suspension is centrifuged for 10 min to remove thick flakes from the monolayers, which are subsequently deposited onto a glass slide and subjected to thermal treatment (250 °C) in a H_2/Ar mixture. The material thus obtained varies in thickness (1-4 graphene layers), though its optical properties match those of graphene generated by micromechanical cleavage.[27] Similarly, graphene monolayers can be prepared by sonication-assisted exfoliation in *N*-methylpyrrolidone.[28]

A bottom-up approach en route to gram-scale production of graphene was envisaged by Stride and associates. Unlike common protocols starting from graphite or other carbon structures, this chemical synthesis of graphene nanosheets use ingredients as cheap as sodium and ethanol, which were reacted in a solvothermal transformation (220 °C, 72 h, sealed vessel) to give a material that was subjected to low-temperature flash pyrolysis followed by gentle sonication.[29] The structure of graphene precursor remains uncertain, although the thermal product is different from pristine metal alkoxide. In fact, no formation of graphene sheets was observed when crystalline sodium ethoxide underwent the solvothermal reaction. It is believed that a metastable ethanol-rich clathrate-like structure could be the actual precursor. The presence of residual sodium and sodium alkoxide would be rapidly dispersed under the action of sound waves. In addition the cavitational energy will be higher in ethanol than in low-boiling solvents.

Single-electron-transfer processes may be triggered by sonication, though the fact remains again largely ignored by practitioners other than sonochemists.[30] In this context, interaction of graphene with electron-donor and electron-acceptor molecules has been investigated, and such a doping modifies the electronic properties of graphene sheets as evidenced by shifts of the G and D bands in Raman spectra.[1]

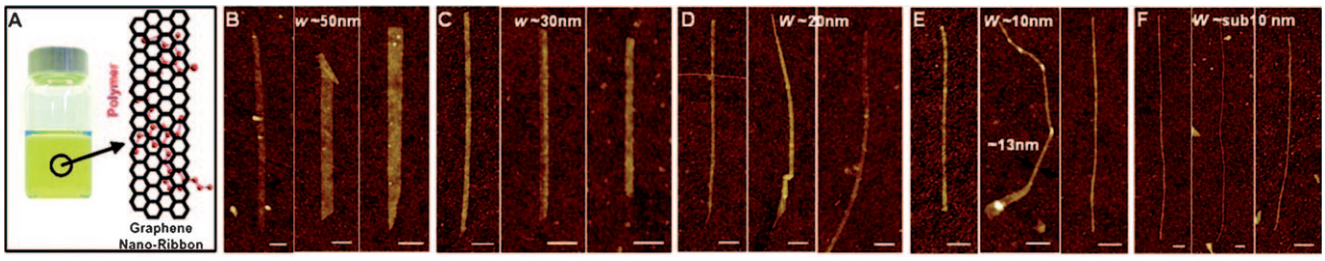

Figure 4. Nanometer-sized graphene nanoribbons (GNRs). A) Solution of PmPV polymer with suspended GNRs. B)–F) show AFM images of GNRs with different widths (scale bars denote 100 nm). In F) the heights of ribbons are approximately 1.5 nm. Reproduced with permission from reference [22]. Copyright 2008 by the American Association for the Advancement of Science.

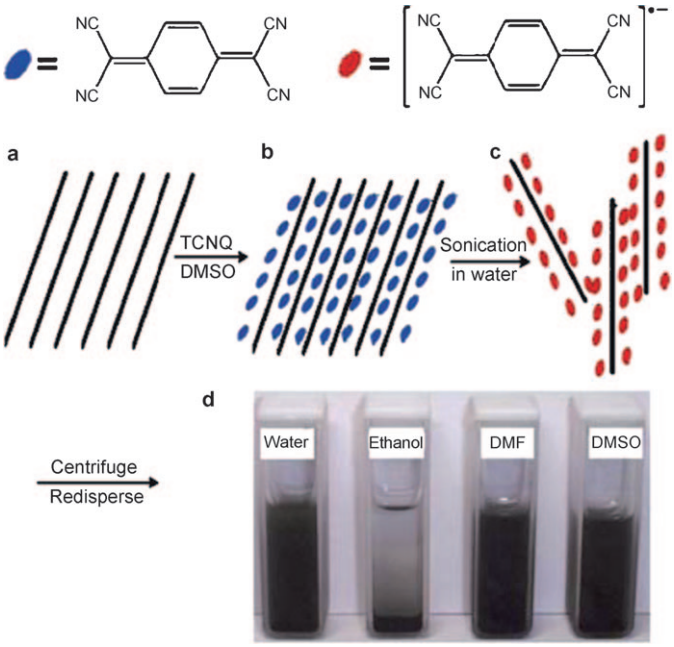

Figure 5. Representation of TCNQ-stabilized graphene dispersions after sonication, and photographs of TCNQ-adsorbed graphene dispersed in various solvents. Reproduced with permission from reference [31]. Copyright 2008 by the Royal Society of Chemistry.

In one of the few reports highlighting molecular charge transfer and sonication in graphene, Hao et al. successfully prepared aqueous dispersions of graphene sheets stabilized by the tetracyanoquinodimethane (TCNQ) anion.[31] Mixing expanded graphite and TCNQ in a mortar with DMSO to favor dissolution of the latter, followed by drying under vacuum and further dispersion in an aqueous solution of KOH under sonication resulted in a black suspension. Single to few-layer graphenes were isolated from the supernatant. Such graphenes incorporating the adsorbed TCNQ anion could also be dispersed in polar aprotic solvents (DMF, DMSO), but not in ethanol (Figure 5).

TEM images reveal not only the existence of isolated sheets, but also of graphene nanoribbons, while electron diffraction images show the six-fold symmetry of the parent graphite (Figure 6). Sonication appears to break mechanically the graphene sheets into small fragments, while leading to individual sheets by disrupting TCNQ intercalation. It should also be conjectured that rapid formation of the TCNQ anion and further adsorption of the ion radical would have been favored by ultrasonic irradiation.

Graphite Oxide: Lamination and Post-Syntheses

As seen before, graphene sheets are susceptible of further molecular decoration, which may affect both the electronic structure and properties, thus enlarging the potential applications of this salient material. These post-synthetic modifications take place by different mechanisms, such as doping; solubilization to afford stable colloidal dispersions; and non-

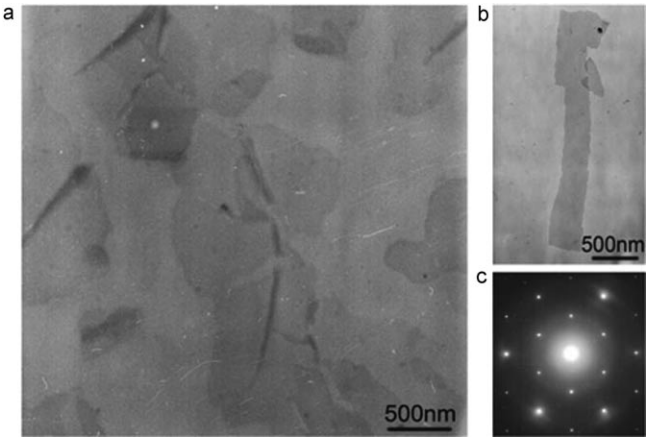

Figure 6. TEM images of a) graphene sheets and b) graphene ribbon, along with c) an electron diffraction pattern photograph. Reproduced with permission from reference [31]. Copyright 2008 by the Royal Society of Chemistry.

covalent functionalization, often with surfactants, and chemical treatments, usually by means of reductive protocols.[1] Unfortunately, the lack of functional groups in graphite itself often hampers facile derivatizations. A more suitable material is graphite oxide (GO), in which oxygen functionalities enable easier chemical modifications than an all-carbon precursor.[32] GO can be synthesized from natural or expandable graphite by the so-called Hummers method or variations thereof,[33] which usually involves treatment with strong mineral acids and an oxidizing agent like $KMnO_4$.

The exact mechanism of GO formation is unclear and, as mentioned earlier, the intermediacy of intercalation derivatives seems quite plausible. It is widely accepted that the final oxidized material contains hydroxy and epoxy groups. A recent study, however, has challenged this homogeneous structure and points to the additional presence of five- and six-membered lactols, as well as quinonoid arrangements. These insights could open the door to alternative functionalizations and reductions yielding more soluble and conductive graphenes.[34] Moreover, a significant amount of sulfur can be incorporated as sulfonic groups in GO prepared by the Hummers methods. The fate of such a sulfur functionality can be monitored by reaction with ammonia.[35]

Previous studies also revealed different levels of oxidation depending on the starting graphite derivative and the oxidative protocol. The corresponding filtrates, supernatants, colloidal dispersions, or isolated solids vary in composition and spectroscopic characteristics.[36] Thus, colloidal suspensions in water produce, after centrifugation, gel-like materials in which the water bound to the GO may accumulate in the pores as well as in the interlayer space. GO particles containing a few layers, plus thicker aggregates, have large average diameters that increased slightly after sonication for 5 min, presumably due to precipitation.

Like graphite, GO exfoliation can be carried out by thermal shock at high temperatures under an inert atmosphere, although stable suspensions can be obtained through less

drastic conditions. Thermal reduction can be conducted by heating GO at 1050 °C with subsequent exfoliation of the stacked structure taking place by extrusion of gas species, most likely CO_2. Enormous pressure (in the MPa range) drives separation of the stacked layers.[37]

Chemical reduction with different reagents followed by dispersion in organic solvents produces graphene monolayers that can be deposited on films or stabilized as graphene colloids. A typical solvothermal reduction of graphene sheets, exfoliated in polar solvents like DMF after ultrasonication, involves treatment with hydrazine hydrate.[38] Different reaction mechanisms have been identified, with the aid of computational methods, for deoxygenation pathways of GO with hydrazine or thermal reduction.[39] Few-layer graphene, generated by oxidation (and/or intercalation) of graphite with H_2SO_4/HNO_3 followed by ultrasonic exfoliation, has also been reduced with hydroquinone at reflux.[40] The crystalline nature of the resulting laminar structure is evidenced by electron diffraction patterns (Figure 7).

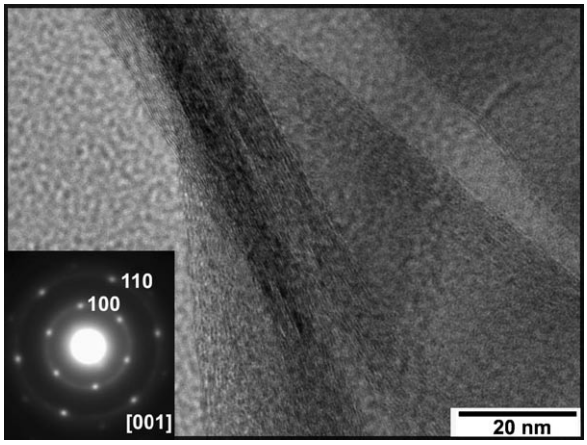

Figure 7. HR-TEM image of a single graphene nanosheet reduced by hydroquinone after sonication. Selected-area electron diffraction pattern evidences its crystalline nature. Reproduced with permission from reference [40]. Copyright 2008 by the American Chemical Society.

Owing to the hydrophilic nature of oxygenated groups, GO can easily be dispersed in water with ultrasound giving rise to very thin graphene oxide sheets. Such sheets, possessing low electrical conductivity, are, however, different from graphitic nanoplatelets or pristine graphene sheets. AFM images of exfoliated GO by ultrasonic treatment revealed the existence of sheets with uniform thickness (ca. 1 nm). Remarkably neither thicker nor thinner sheets were observed, thus suggesting the formation of single layers of GO under this treatment (Figure 8). Further reduction with hydrazine hydrate produces an electrically conductive material consisting of aggregated graphene sheets. Although reduction does not completely remove oxygen functionalities, the modified GO is less hydrophilic. Unfortunately, re-dispersion in water or stable dispersions in a number of different organic solvents could not be attained.[41]

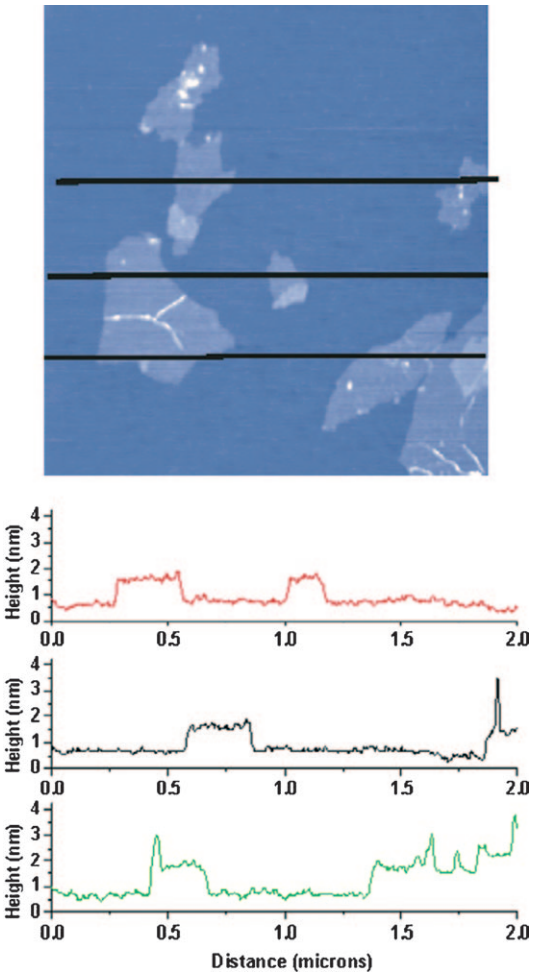

Figure 8. AFM image of GO exfoliated by ultrasonic treatment and height profiles obtained in different locations. Reproduced with permission from reference [41]. Copyright 2007 by Elsevier Ltd.

Ruoff et al. have devised a general strategy toward graphene-based composites by treating GO with organic isocyanates.[42] The isocyanate treatment enhances the hydrophobic character of GO by producing amide and carbamate linkages to carboxy and hydroxy groups, respectively, present at the GO surface. The functionalized material no longer exfoliates in water, but forms stable dispersions in polar aprotic solvents. Such dispersions can be obtained after ultrasonic treatment of PhNCO-treated GO (150 W, 1 h). AFM images reveal again the presence of individual GO sheets with thickness of about 1 nm. Polymer composites are then generated by mixing these dispersions with a variety of macromolecules: polystyrene, styrene–butadiene, or acrylonitrile–butadiene–styrene copolymers, followed by chemical reduction with dimethyl hydrazine (at 80 °C for 24 h).[42b] This reduction step is critical to induce electrical conductivity; moreover, the presence of the polymer in solution also prevents the agglomeration of sheets.

An interesting material, graphene oxide paper, is readily obtained by flow-directed assembly of individual sheets.[43] Colloidal dispersions of graphene oxide sheets (20 mL

batches with concentrations of 3 mg mL^{-1}) are formed by means of ultrasonication in a cleaning bath. Filtration of the resulting colloid through a membrane filter (47 mm in diameter, 0.2 μm pore size) followed by air drying and peeling from the filter results in graphene oxide paper samples, the thickness of which can be controlled by adjusting the volume of the suspension. Samples thus obtained can be cut without structural damage and are superior in mechanical properties (in terms of tensile modulus and fracture strength) than other inorganic paperlike materials.[44] Inorganic composites can be generated by dispersing metal particles or metal oxides onto graphene nanosheets, with sonication favoring both exfoliation and formation of the stable colloidal nanocomposite.[45] SEM images of the graphene paper reveal densely packed layers. Further X-ray diffraction analysis evidences the layering of the graphene oxide paper with an average interlayer distance (*d*-spacing) of 0.83 nm. The stack of graphene oxide sheets (oriented perpendicularly to the diffracting plane) in the paper corresponds approximately to 5.2 nm (Figure 9).

A plethora of chemical treatments to modify graphene oxide sheets have been recently introduced. Current trends are directed to replace toxic reagents (like hydrazines) by greener surrogates as well as to incorporate more elaborated functionalities, thereby improving both mechanical and electrical properties.[1] In a recent variation, Ma et al. have demonstrated that graphene monolayers can be stabilized for long times in a volatile solvent like ethanol after reduction with *p*-phenylenediamine and mild ultrasonication. Graphene films subsequently formed by electrophoretic deposition on indium tin oxide-coated glass exhibit high conductivity.[46]

A different, organic approach to GO followed by mild reduction also provides new vistas into the formation of graphene oxide sheets and reduced nanoplatelets.[47] Here, a solvent-free protocol involving heating (at 110 °C) of graphite and low-melting benzoyl peroxide (BPO) produces GO within 10 min, which can be dispersed in water by sonication. Reduction was accomplished by treatment with $NaBH_4$ at 125 °C for 3 h. Stable colloidal suspensions of both graphene oxide and reduced graphene oxide are obtained with ultrasound (at an intensity of 450 W for 300 s) as revealed by AFM images (Figure 10). Isolated sheets of the exfoliated graphene oxide have an average thickness of ≈1.3 nm, while the reduced nanoplatelets display height variations of about 1.5 nm on average, suggesting that exfoliation down to one to three layers is generated by the ultrasonic treatment.

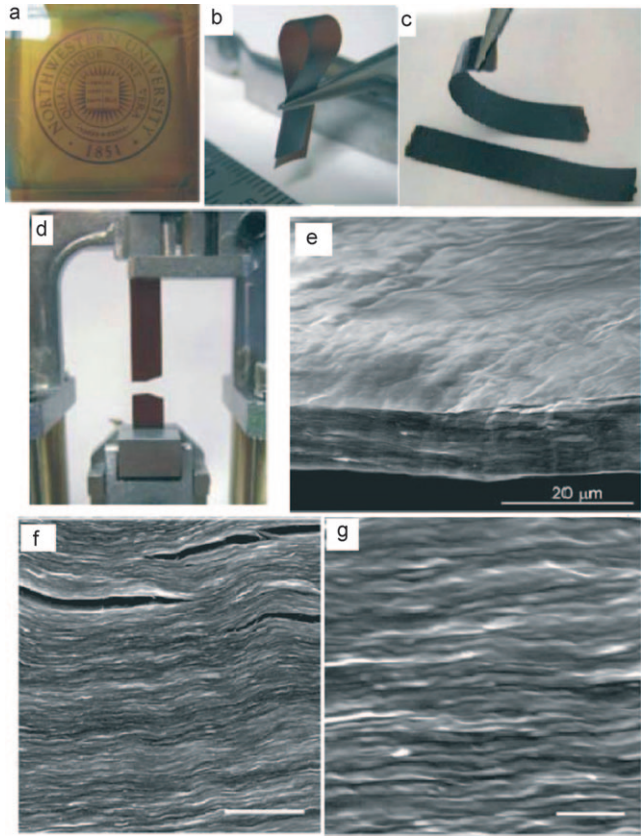

Figure 9. Morphology and properties of graphene oxide paper: a) shows a logo beneath the paper (≈1 μm thick); b) folded ≈5 μm-thick transparent film; c) folded ≈25 μm-thick strip; d) strip after fracture by tensile stress; e)–g) show SEM images of ≈10 μm-thick samples at different resolutions; the scale bars in f) and g) are 2 μm and 250 nm, respectively. Reproduced with permission from reference [43] Copyright 2007 by Macmillan Publishers Ltd.

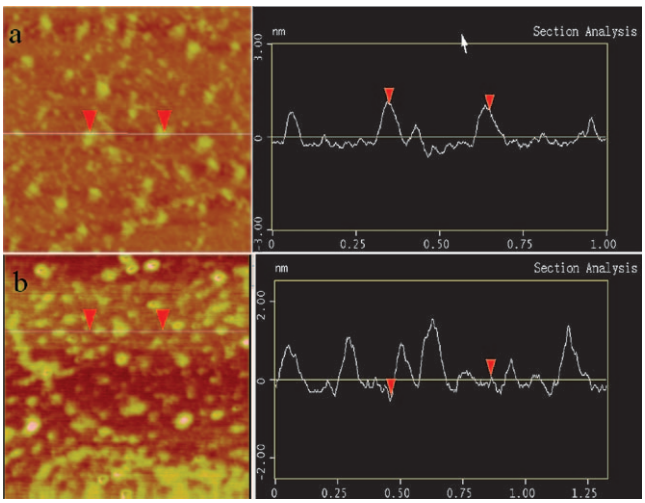

Figure 10. AFM images of a) graphene oxide and b) reduced graphene oxide nanoplatelets with the corresponding height profiles. Reproduced with permission from reference [47]. Copyright 2009 by the American Chemical Society.

The authors have speculated that the reaction mechanism under these conditions could involve three steps as depicted in Figure 11. Thus, edge-to-face noncovalent aromatic interactions between a graphene surface and BPO might primarily lead to intercalation between adjacent nanosheets. Then, decomposition of BPO upon heating also favors exfoliation with concomitant release of gas molecules and free radicals (in fact XRD analysis reveals an increase of the *d*-spacing from 0.34 to 0.78 nm). Finally, free radicals may react with

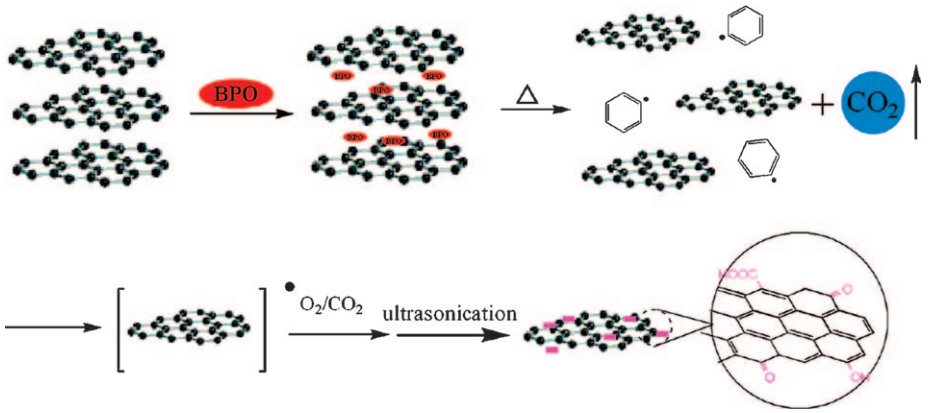

Figure 11. Proposed mechanism of graphene oxide production with benzoyl peroxide under sonication. Reproduced with permission from reference [47]. Copyright 2009 by the American Chemical Society.

oxygen and CO_2 to produce GO, which in water under sonication converts into graphene oxide.[47] The authors leave open the question of how radical species would react with oxygen and other volatile species. Clearly their analysis overlooks the role of cavitation as presumably electron-transfer processes are enhanced by sonication, and interaction of radical species coming from water sonolysis would contribute to the formation of the oxygenated graphitic surface, which in turn further exfoliates under the mechanical action of sound waves.

Although reactive radicals from peroxide decomposition should play an important role in producing CO_2; formation of the latter in carbon materials has recently emerged as a puzzling question. In a very recent computational study, Radovic has scrutinized the simple reaction of $C+(1-y/2)O_2 \rightarrow (1-y)CO_2+yCO$. The proposed mechanism clarifies the adsorption and reactivity of molecular oxygen on the surface of sp^2-hybridized carbons. The results point to reactive sites at graphene edges as carbene- and carbyne-like carbon atoms.[48]

A practical and convenient oxidation protocol that uncovers the multiple and positive effects of sonication has been presented recently.[49] Large-sized single-layer graphene oxide sheets (up to several mm^2) can be obtained by a modification of the classical Hummers' method in which the first oxidation is replaced by sonication in concentrated H_2SO_4 solutions. The treatment fragments graphite flakes into smaller and thinner particles. Graphene oxide monolayers were subsequently obtained by room-temperature oxidation with $H_2SO_4/KMnO_4$. The authors found that the lateral size of such monolayers could be better controlled by adjusting the sonication period. Irradiation for 1 h results in ultralarge sheets (up to 3 mm), whereas sonication for 2 h produces sheets ranging from 50 to 100 μm in lateral size (Figure 12). Smaller flakes (less than 10 μm) were obtained after 6 h of sonication. After chemical (hydrazine hydrate) or thermal reduction (H_2/Ar), the nanosheets were employed as conducting thin-film electrodes. The transistor devices made from the monolayers after reduction at 800 °C showed enhanced hole mobility, which correlates with graphitization of graphene oxide rather than elimination of the oxygenated functions.

More elaborated molecular decorations can be achieved by well-established chemistry. In a recent example, conducting graphene platelets were obtained from ultrasound-assisted exfoliation of GO, then treated with NaN_3, and further reduction with $LiAlH_4$ lead to amino-functionalized GO.[50] In subsequent derivatizations, assisted by sonication, GO-NH_2 was attached to an isothiocyanate monolayer on a SiO_2 surface resulting in thioureido linkages (Figure 13).

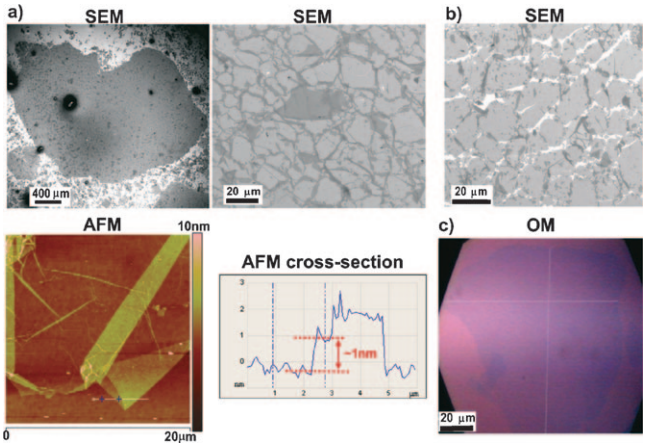

Figure 12. a) SEM and AFM images of large graphene oxide sheets on quartz (sonication in H_2SO_4 for 1 h). b) SEM image of graphene oxide after reduction at 800 °C. c) Optical micrograph of the nanosheets after 2 h sonication. Reproduced with permission from reference [49]. Copyright 2009 by the American Chemical Society.

Alternatively GO-N_3 can be subjected to click coupling with a long-chain alkyne. Single sheets with 1 nm thickness could be visualized by both AFM and TEM images (Figure 14). Since the Cu-catalyzed azide–alkyne cycloaddition is orthogonal with cell chemistry, this and related functionalizations of graphene derivatives may give rise to new carbon-doped biomaterials.

Another polyvalent GO, with both exfoliation and post-synthetic modification assisted by sonication, involves a one-step preparation of GO/magnetic-nanoparticle composites.[51] This decoration is accomplished by treating GO dispersed in *N*-methylpyrrolidone with iron(III) triacetylacetonate. The same ultrasonication conditions were unsuccessful to exfoliate the original graphite. The nanoparticles act as spacers disrupting the formation of a stacked structure. Separation of the resulting magnetic GO in water could be easily achieved with an external magnet.

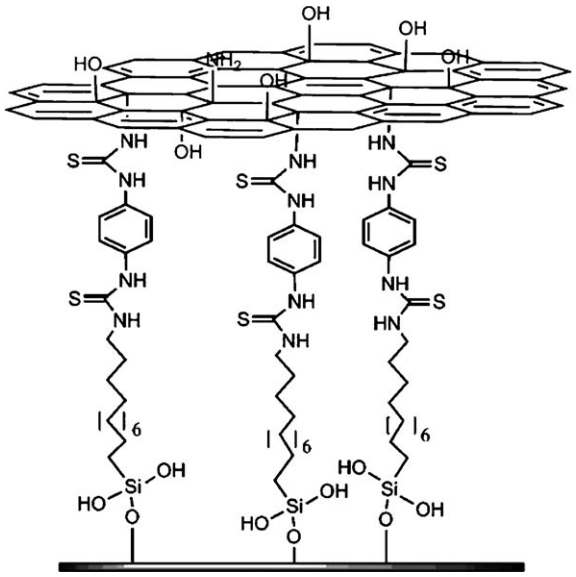

Figure 13. Putative structure of the GO-NH_2 layers covalently attached to a silicon-based substrate via thioureido linkages. Reproduced with permission from reference [50]. Copyright 2009 by Wiley-VCH Verlag GmbH & Co. KGaA.

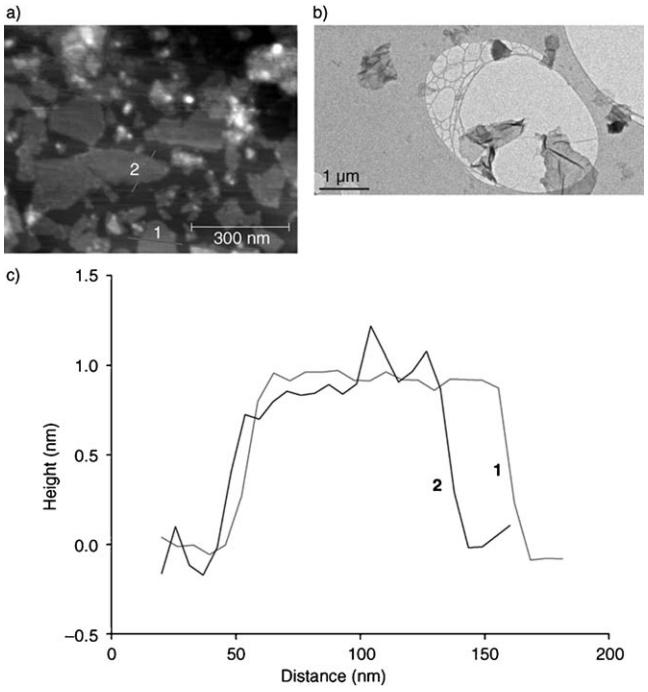

Figure 14. a) AFM and b) TEM images of a GO-triazole monolayer (GO-C_{18}) obtained by Cu-catalyzed Huisgen cycloaddition; c) represents the cross sections of the AFM image showing the height profile. Reproduced with permission from reference [50]. Copyright 2009 by Wiley-VCH Verlag GmbH & Co. KGaA.

Carbon Allotropes: A Dynamic View

As discussed above unzipping of carbon nanotubes (CNTs) by chemical and solvothermal methods offers viable routes to graphene sheets. Since rational syntheses of discrete all-carbon molecules (e.g., fullerenes) can be achieved by condensation of polycyclic aromatic hydrocarbons (PAHs),[52] these polyaromatic species could equally serve as both precursors and intermediates of complex carbon structures. Like fullerenes, the de novo production of CNTs is complex and evidently unpractical on a large scale. A research team has gratifyingly invented an alternative catalyst-free wet strategy based on the fact that inexpensive graphitic precursors may decompose into PAHs under appropriate conditions.[53] A facile and mild room-temperature treatment of GO with 70% HNO_3 under sonication leads to carbon nanotubes and nanoribbons, along with fullerene-like particles. Ultrasound irradiation is capable of fragmenting the GO nanosheets, which, under cavitation, further nucleate and self-assemble into different carbon structures (Figure 15), a process resembling sonocrystallization.

Generation of PAHs could be ascertained by time-dependent mass spectrometry analysis with samples further checked by microscopy techniques (Figure 16). The CNTs have crystalline walls with outer diameters of 5–20 nm (and inner ones between 2–7 nm) and lengths in the wide range of 30–135 nm.

The role of sonication is indeed crucial as cavitation produces sufficient strain and friction forces in the liquid to cause bond fracture in the carbon framework. Prolonged sonication also favors formation of rolled-up and highly curved structures that are more resistant to cutting. Remarkably, the authors observed the sonochemical fate at different temperatures, which agrees with the fact that cavitation is influenced by the macroscopic temperature of the bulk solution. Thus, more microbubbles are generated at higher temperature, which hinder the propagation of ultrasound waves. While sonication at room temperature favors the acid-catalyzed inter- and intramolecular dehydration reactions of the aromatic fragments, increasing the temperature above 60°C did not result in CNT formation and only fullerene particles were detected. Above 70°C, the cavitational energy was insufficient to promote chemical organization and only amorphous carbon was produced in the poorly volatile aqueous medium.

This research appears to be consistent with recent findings on the effect of high-power ultrasound (probes at 19.7 kHz and 500 W of maximal power) on bulk graphite producing a myriad of down-scaling fragmentations, which include damaged nanosheets and aromatics.[54] Previous studies had also shown that C_{60} and CNTs, though in minute amounts, can be assembled from aromatics under ultrasound (Ti probe) in solution.[55]

Owing to their two-dimensional structure with existing defects, GO sheets easily undergo transformation (10 min sonication).[53] In contrast, the acid-catalyzed fragmentation of SWCNTs under sonication takes longer at higher temperature.[56] In the present context, SWCNTs are readily dispersed through sonication in halocarbon solvents, although solvent decomposition is substantially responsible of post-synthetic modifications and doping of the nanotubes.[57]

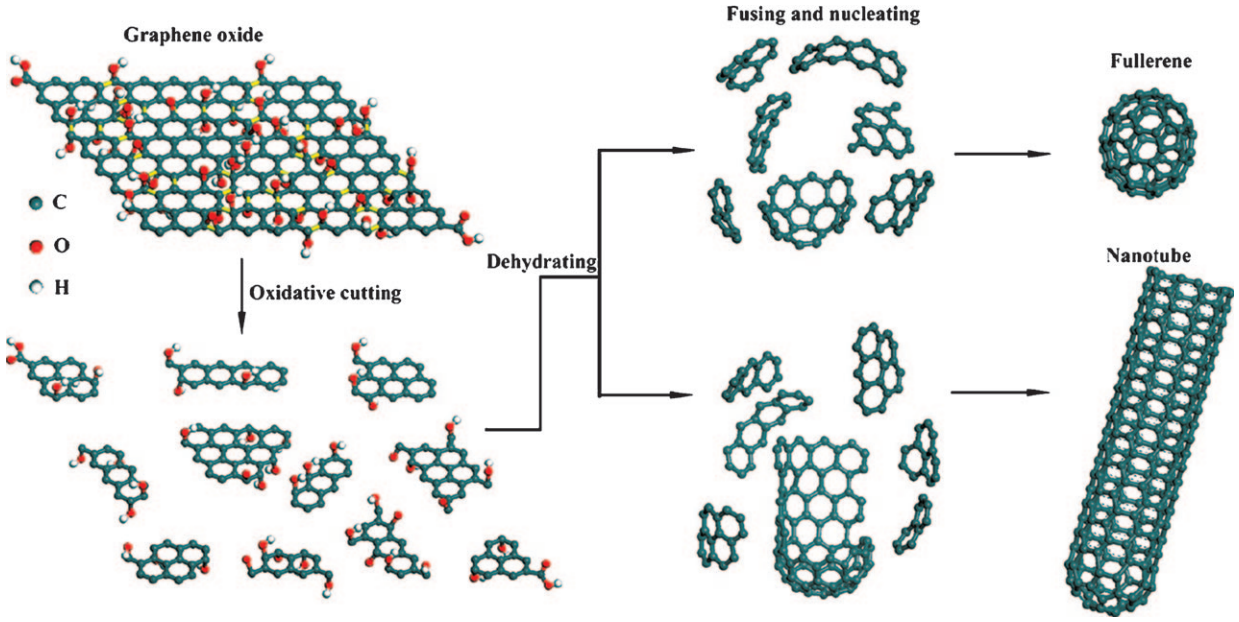

Figure 15. Scheme illustrating a possible mechanism for converting graphene oxide nanosheets into CNTs and carbon particles under sonication in HNO_3. Reproduced with permission from reference [53]. Copyright 2009 by the American Chemical Society.

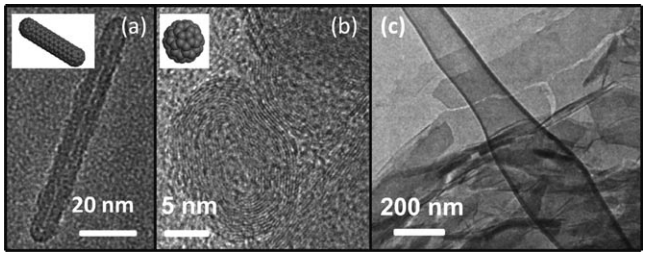

Figure 16. TEM images of a) a carbon nanotube, b) carbonaceous particles, and c) carbon nanoribbons generated from graphene oxide by RT sonication in HNO_3. Reproduced with permission from reference [53]. Copyright 2009 by the American Chemical Society.

SWCNT bundles, however, when sonicated in dilute *N*-methylpyrrolidone have been shown to disperse and exfoliate. The process is unusual in that the entropy term of mixing for such large molecules is very small; in other words the situation represents true thermodynamic solubility with an enthalpy of mixing near zero or even negative. STM images after sonication showed evidence of solvent molecules adsorbed on the SWCNTs migrating from inside the bundles to the deposition surface. Thus, this physisorption onto the carbon surfaces drives solubilization.[58]

Accurate studies on the mechanism of cavitation-induced fragmentation and dispersion of carbonaceous materials are still scarce and most usually ignore the science behind sound waves.[8] Studies so far have been focused on CNTs, though they are instrumental in developing useful and reproducible protocols. Sonication may effectively cut polymers into shorter fragments.[59] Dispersed SWCNTs when subjected to a further ultrasonic treatment tend to separate by tube length and diameter.[60] Hennrich et al. have investigated the sonochemical scission of SWCNTs using an ultrasonic probe (20 kHz, 200 W at 10% power) in the presence of a surfactant (sodium cholate).[14] Applying a continuum model and modeling bubble dynamics by means of the well-known Rayleigh-Plesset equation, the team was able to relate the net force at the nanotube with the length distribution, the strain rate, and the fluid viscosity. The maximum of the tube length distribution (L_M) shows a dependence on the sonication time (t), roughly as $L_M \approx t^{-0.5}$, which agrees with experimental figures, although deviations are observed at shorter irradiation times. However, as noted in an earlier section of this minireview, the forces acting on a tube or fiber near an imploding microbubble are not easy to model. A recent study has actually challenged the above conclusions pointing to an average length that scales as $L_M \approx t^{-n}$, with $n \approx 0.2$, and suggesting that CNTs could be broken into very small pieces after prolonged sonication.[61] It would also possible that the nanotubes could be cut layer-by-layer on the basis of the weak interactions between adjacent graphene layers. However, the authors did not observe substantial diameter reductions under their experimental conditions and ruled out this mechanism governing the scission of the tubes. Probably, structural defects at the graphene layers would increase the intermolecular interactions, thereby limiting layer scission still further. As pointed out, a turbulent flow cannot be discarded either,[15] although it is unclear if turbulence has enough time to develop around a collapsing bubble. Moreover, these studies start from spherical models for the microbubble, which would hardly occur near a solid surface.[11] Anyway, these considerations appear to be promising to rationalize the forces exerted on carbon sheets by an ultrasonic field.

Conclusion and Outlook

Sonication has become an indispensable tool to exfoliate graphitic materials and leading to stable colloids under mild conditions; this constitutes the core protocol in wet chemistry to fabricate graphene-type nanosheets. In addition, irradiation also facilitates solubilization and post-synthetic reductive transformations giving rise to functionalized graphenes. Although the method produces variable results, depending on the experimental conditions, it is simple, largely reproducible, safe, and available to most laboratories; it circumvents the risks and drawbacks of gas-phase or solvothermal reactions conducted at high temperatures.

Still we need to fill a knowledge gap, as sonication is viewed rather as a laboratory trick and not a physical irradiation influenced by numerous parameters and solvent properties. It is therefore surprising how most transformations are conducted in cleaning baths, in which neither optimal intensity nor temperature can be controlled with accuracy. Moreover, an increase in temperature may result in further damage and uncontrolled aggregation. Probes, usually operating at 20 kHz, with greater power densities ($W cm^{-2}$), external cooling and/or pulsed irradiation, are more desirable and reproducible. A combined pre-treatment of sonication to cause exfoliation, followed by a faster reductive decoration (e.g. with microwaves), resulting in single or few layers of graphene,[62] will also open the door to more selective processes.

Through this minireview we have highlighted the complex, yet predictable, interactions of an acoustic field with a layered material. Sound waves undergo attenuation and cause plastic stress and deformations, which will be enhanced by cavitational implosion. The rationale has been, and will doubtless be, extended to other carbonaceous and layered structures. Conductive materials can be obtained by sonicating or grinding carbon nanotubes in ionic liquids, media with almost negligible volatility in which cavitation would hardly take place.[63] Likewise, zeolites can easily be delaminated by ultrasound irradiation,[64] and sonication also promotes the organization of zeolite microcrystals into 2D and 3D microstructures.[65]

Thus, even though sonication-free dissolution methods have been introduced for the production of graphene sheets and ribbons,[66] the versatility of sound waves represent simple and clean routes to exfoliate and disperse large flakes and to produce functional composites.[67] Extensions to other layered materials, such as boron nitride,[68] set new directions and potentialities in innovative materials. Finally, the usual hurdle of working out and distinguishing between samples of various thicknesses (as the properties of graphenes are significantly dependent on the layer number) could be solved at last by coating and microscopy-based methods.[69,70]

Acknowledgements

Financial support from the Spanish Ministry of Science and Innovation (Grant MAT2009-14695-C04-01), the University of Turin and Regione Piemonte (Project NanoSAFE-2006) are gratefully acknowledged. We also thank the European Union for supporting our research program on applications of high-intensity ultrasound and microwaves through the COST Action D32/006/04 over recent years. Lastly, special thanks go to César Cintas and Francisco Prados for designing the frontispiece of this article.

[1] For recent and authoritative reviews, see: a) M. J. Allen, V. C. Tung, R. B. Kaner, *Chem. Rev.* **2010**, *110*, 132–145; b) A. K. Geim, *Science* **2009**, *324*, 1530–1534; c) C. N. R. Rao, A. K. Sood, K. S. Subrahmanyam, A. Govindaraj, *Angew. Chem.* **2009**, *121*, 7890–7916; *Angew. Chem. Int. Ed.* **2009**, *48*, 7752–7777; d) T. Ando, *NPG Asia Mater.* **2009**, *1*, 17–21; e) M. Taghioskoui, *Mater. Today* **2009**, *12(10)*, 34–37.
[2] X. K. Lu, H. Huang, M.-F. Yu, R. Ruoff, *Chem. Eng. News* **2009**, *87(17)*, p. 2.
[3] a) X. K. Lu, H. Huang, N. Nemchuk, R. S. Ruoff, *Appl. Phys. Lett.* **1999**, *75*, 193–195; b) X. K. Lu, M.-F. Yu, H. Huang, R. S. Ruoff, *Nanotechnology* **1999**, *10*, 269–272.
[4] a) K. S. Novoselov, A. K. Geim, S. V. Morozov, D. Jiang, Y. Zhang, S. V. Dubonos, I. V. Grigorieva, A. A. Firsov, *Science* **2004**, *306*, 666–669; b) K. S. Novoselov, D. Jiang, F. Schedin, T. J. Booth, V. V. Khotkevich, S. V. Morozov, A. K. Geim, *Proc. Natl. Acad. Sci. USA* **2005**, *102*, 10451–10453.
[5] Ultraflat graphene (with height variations less than 25 pm as detected by AFM) has been recently produced by deposition of mechanically exfoliated graphite sheets on atomically flat terraces of mica surfaces: C. H. Lui, L. Liu, K. F. Mak, G. W. Flynn, T. F. Heinz, *Nature* **2009**, *462*, 339–341.
[6] A. Dato, Z. Lee, K.-J. Jeon, R. Erni, V. Radmilovic, T. J. Richardson, M. Frenklach, *Chem. Commun.* **2009**, 6095–6097.
[7] a) X. Y. Yang, X. Dou, A. Rouhanipour, L. J. Zhi, H. J. Rader, K. Mullen, *J. Am. Chem. Soc.* **2008**, *130*, 4216–4217; b) W. Zhang, J. Cui, C. Tao, Y. Wu, Z. Li, L. Ma, Y. Wen, G. Li, *Angew. Chem.* **2009**, *121*, 5978–5982; *Angew. Chem. Int. Ed.* **2009**, *48*, 5864–5868.
[8] S. E. Skrabalak, *Phys. Chem. Chem. Phys.* **2009**, *11*, 4930–4942, and references therein.
[9] R. E. Newnham, *Properties of Materials. Anisotropy, Symmetry, Structure*, Oxford University Press, Oxford, **2005**, pp. 249–260.
[10] R. E. Newnham, B. A. Auld, *Acoustic Fields and Waves in Solids*, Krieger, Malabar, **1990**.
[11] T. J. Mason, *Practical Sonochemistry. User's Guide to Applications in Chemistry and Chemical Engineering*, Ellis Horwood, London, **1991**, pp. 27–28.
[12] G. Cravotto, P. Cintas, *Chem. Soc. Rev.* **2006**, *35*, 180–196.
[13] J. A. Odell, A. Keller, Y. Rabin, *J. Chem. Phys.* **1988**, *88*, 4022–4028.
[14] F. Hennrich, R. Krupke, K. Arnold, J. A. R. Stütz, S. Lebedkin, T. Koch, T. Schimmel, M. M. Kappes, *J. Phys. Chem. B* **2007**, *111*, 1932–1937.
[15] S. A. Vanapalli, S. L. Ceccio, M. J. Solomon, *Proc. Natl. Acad. Sci. USA* **2006**, *103*, 16660–16665.
[16] K. L. Lu, R. M. Lago, Y. K. Chen, M. L. H. Green, P. J. F. Harris, S. C. Tsang, *Carbon* **1996**, *34*, 814–816.
[17] Z. Wang, L. Yu, W. Zhang, Z. Zhu, G. He, Y. Chen, G. Hu, *Phys. Lett. A* **2003**, *307*, 249–252.
[18] Q. Li, X. Zhang, G. Wu, S. Xu, C. Wu, *Ultrason. Sonochem.* **2007**, *14*, 225–228.
[19] J. E. Jones, M. C. Cheshire, D. J. Casadonte, Jr., C. C. Phifer, *Org. Lett.* **2004**, *6*, 1915–1917.
[20] J. Walter, M. Nishioka, S. Hara, *Chem. Mater.* **2001**, *13*, 1828–1833.
[21] a) L. M. Viculis, J. J. Mack, R. B. Kaner, *Science* **2003**, *299*, 1361; b) L. M. Viculis, J. J. Mack, O. M. Mayer, H. T. Hahn, R. B. Kaner, *J. Mater. Chem.* **2005**, *15*, 974–978.

[22] X. Li, X. Wang, L. Zhang, S. Lee, H. Dai, *Science* **2008**, *319*, 1229–1232.
[23] L. Jiao, L. Zhang, X. Wang, G. Diankov, H. Dai, *Nature* **2009**, *458*, 877–880.
[24] D. V. Kosynkin, A. L. Higginbotham, A. Sinitskii, J. R. Lomeda, A. Dimiev, B. K. Price, J. M. Tour, *Nature* **2009**, *458*, 872–876.
[25] Q. Li, Y. Ma, C. Mao, C. Wu, *Ultrason. Sonochem.* **2009**, *16*, 752–757.
[26] X. Li, G. Zhang, X. Bai, X. Sun, X. Wang, E. Wang, H. Dai, *Nat. Nanotechnol.* **2008**, *3*, 538–542.
[27] P. Blake, P. D. Brimicombe, R. R. Nair, T. J. Booth, D. Jiang, F. Schedin, L. A. Ponomarenko, S. V. Morozov, H. F. Gleeson, E. W. Hill, A. K. Geim, K. S. Novoselov, *Nano Lett.* **2008**, *8*, 1704–1708.
[28] Y. Hernandez, V. Nicolosi, M. Lotya, F. M. Blighe, Z. Sun, S. De, I. T. McGovern, B. Holland, M. Byrne, Y. K. Gunko, J. J. Boland, P. Niraj, G. Duesberg, S. Krishnamurthy, R. Goodhue, J. Hutchinson, V. Scardaci, A. C. Ferrari, J. N. Coleman, *Nat. Nanotechnol.* **2008**, *3*, 563–568.
[29] M. Choucair, P. Thordarson, J. A. Stride, *Nat. Nanotechnol.* **2009**, *4*, 30–33.
[30] M. Chanon, J.-L. Luche, *Synthetic Organic Sonochemistry* (Ed.: J.-L. Luche), Plenum Press, New York, **1998**, pp. 376–392.
[31] R. Hao, W. Qian, L. Zhang, Y. Hou, *Chem. Commun.* **2008**, 6576–6578.
[32] For a recent and comprehensive revision on the chemistry of graphene oxide, see: D. R. Dreyer, S. Park, C. W. Bielewski, R. S. Ruoff, *Chem. Soc. Rev.* **2010**, *39*, 228–240, and references therein.
[33] W. S. Hummers, Jr., R. E. Offeman, *J. Am. Chem. Soc.* **1958**, *80*, 1339.
[34] W. Gao, L. B. Alemany, L. Ci, P. M. Ajayan, *Nat. Chem.* **2009**, *1*, 403–408.
[35] C. Petit, M. Seredych, T. J. Bandosz, *J. Mater. Chem.* **2009**, *19*, 9176–9185.
[36] G. I. Titelman, V. Gelman, S. Bron, R. L. Khalfin, Y. Cohen, H. Bianco-Peled, *Carbon* **2005**, *43*, 641–649.
[37] a) H. C. Schniepp, J.-L. Li, M. J. McAllister, H. Sai, M. Herrera-Alonso, D. H. Adamson, R. K. Prud′homme, R. Car, D. A. Saville, I. A. Aksay, *J. Phys. Chem. B* **2006**, *110*, 8535–8539; b) M. J. McAllister, J.-L. Li, D. H. Adamson, H. C. Schniepp, A. A. Abdala, J. Liu, M. Herrera-Alonso, D. L. Milius, R. Car, R. K. Prud′homme, I. A. Aksay, *Chem. Mater.* **2007**, *19*, 4396–4404.
[38] H. Wang, J. T. Robinson, X. Li, H. Dai, *J. Am. Chem. Soc.* **2009**, *131*, 9910–9911.
[39] X. Gao, J. Jang, S. Nagase, *J. Phys. Chem. C* **2010**, 114, 832–842.
[40] G. Wang, J. Yang, J. Park, X. Guo, B. Wang, H. Liu, J. Yao, *J. Phys. Chem. C* **2008**, *112*, 8192–8195.
[41] S. Stankovich, D. A. Dikin, R. D. Piner, K. A. Kohlhaas, A. Kleinhammes, Y. Jia, Y. Wu, S. T. Nguyen, R. S. Ruoff, *Carbon* **2007**, *45*, 1558–1565.
[42] a) S. Stankovich, R. D. Piner, S. T. Nguyen, R. S. Ruoff, *Carbon* **2006**, *44*, 3342–3347; b) S. Stankovich, D. A. Dikin, G. H. B. Dommett, K. M. Kohlhaas, E. J. Zimney, E. A. Stach, R. D. Piner, S. T. Nguyen, R. S. Ruoff, *Nature* **2006**, *442*, 282–286.
[43] D. A. Dikin, S. Stankovich, E. J. Zimney, R. D. Piner, G. H. B. Dommett, G. Evmenenko, S. T. Nguyen, R. S. Ruoff, *Nature* **2007**, *448*, 457–460.
[44] D. G. H. Ballard, G. R. Rideal, *J. Mater. Sci.* **1983**, *18*, 545–561.
[45] See for instance: T. N. Lambert, C. A. Chavez, B. Hernandez-Sanchez, P. Lu, N. S. Bell, A. Ambrosini, T. Friedman, T. J. Boyle, D. R. Wheeler, D. L. Huber, *J. Phys. Chem. C* **2009**, *113*, 19812–19823, and references therein.
[46] Y. Chen, X. Zhang, P. Yu, Y. Ma, *Chem. Commun.* **2009**, 4527–4529.
[47] J. Shen, Y. Hu, M. Shi, X. Lu, C. Qin, C. Li, M. Ye, *Chem. Mater.* **2009**, *21*, 3514–3520.
[48] L. R. Radovic, *J. Am. Chem. Soc.* **2009**, *131*, 17166–17175.
[49] C.-Y. Su, Y. Xu, W. Zhang, J. Zhao, X. Tang, C.-H. Tsai, L.-J. Li, *Chem. Mater.* **2009**, *21*, 5674–5680.
[50] R. Salvio, S. Krabbenborg, W. J. M. Naber, A. H. Velders, D. N. Reinhoudt, W. G. van der Wiel, *Chem. Eur. J.* **2009**, *15*, 8235–8240.
[51] J. Shen, Y. Hu, M. Shi, N. Li, H. Ma, M. Ye, *J. Phys. Chem. C* **2010**, *114*, 1498–1503.
[52] a) L. T. Scott, M. M. Boorum, B. J. McMahon, S. Hagen, J. Mack, J. Blank, H. Wegner, A. de Meijere, *Science* **2002**, *295*, 1500–1503; b) G. Otero, G. Biddau, C. Sánchez-Sánchez, R. Caillard, M. F. López, C. Rogero, F. J. Palomares, N. Cabello, M. A. Basanta, J. Ortega, J. Méndez, A. M. Echavarren, R. Pérez, B. Gómez-Lor, J. A. Martín-Gago, *Nature* **2008**, *454*, 865–868.
[53] S. Wang, L. A. I. Tang, Q. Bao, M. Lin, S. Deng, B. M. Goh, K. P. Loh, *J. Am. Chem. Soc.* **2009**, *131*, 16832–16837.
[54] F. Guittonneau, A. Abdelouas, B. Grambow, S. Huclier, *Ultrason. Sonochem.* **2010**, *17*, 391–398.
[55] a) R. Katoh, E. Yanase, H. Yokoi, S. Usuba, Y. Kakudate, S. Fujiwara, *Ultrason. Sonochem.* **1998**, *5*, 37–38; b) R. Katoh, Y. Tasaka, E. Sekreta, M. Yumura, F. Ikazaki, Y. Kakudate, S. Fujiwara, *Ultrason. Sonochem.* **1999**, *6*, 185–187; c) S. H. Jeong, J. H. Ko, J. B. Park, W. Park, *J. Am. Chem. Soc.* **2004**, *126*, 15982–15983.
[56] K. J. Ziegler, Z. N. Gu, H. Q. Peng, E. L. Flor, R. H. Hauge, R. E. Smalley, *J. Am. Chem. Soc.* **2005**, *127*, 1541–1547.
[57] K. R. Moonoosawmy, P. Kruse, *J. Am. Chem. Soc.* **2008**, *130*, 13417–13424.
[58] S. D. Bergin, V. Nicolosi, P. V. Streich, S. Giordani, Z. Sun, A. H. Windle, P. Ryan, N. P. P. Niraj, Z.-T. T. Wang, L. Carpenter, W. J. Blau, J. J. Boland, J. P. Hamilton, J. N. Coleman, *Adv. Mater.* **2008**, *20*, 1876–1881.
[59] M. W. A. Kuijpers, P. D. Iedema, M. F. Kemmere, J. T. F. Keurentjes, *Polymer* **2004**, *45*, 6461–6467.
[60] D. A. Heller, R. M. Mayrhofer, S. Baik, Y. V. Grinkova, M. L. Usrey, M. S. Strano, *J. Am. Chem. Soc.* **2004**, *126*, 14567–14573.
[61] A. Lucas, C. Zakri, M. Maugey, M. Pasquali, P. van der Schoot, P. Poulin, *J. Phys. Chem. C* **2009**, *113*, 20599–20605.
[62] A. V. Murugan, T. Muraliganth, A. Manthiram, *Chem. Mater.* **2009**, *21*, 5004–5006.
[63] a) T. Fukushima, T. Aida, *Chem. Eur. J.* **2007**, *13*, 5048–5058; b) Z. Lin, J. R. Lomeda, B. K. Price, W. Lu, Y. Zhu, J. M. Tour, *Chem. Mater.* **2009**, *21*, 3045–3047.
[64] M.-A. Springuel-Huet, F. Guenneau, A. Gédéon, A. Corma, *J. Phys. Chem. C* **2007**, *111*, 5694–5700.
[65] K. B. Yoon, *Acc. Chem. Res.* **2007**, *40*, 29–40, and references therein.
[66] C. Vallés, C. Drummond, H. Saadaoui, C. A. Furtado, M. He, O. Roubeau, L. Ortolani, M. Monthioux, A. Pénicaud, *J. Am. Chem. Soc.* **2008**, *130*, 15802–15804.
[67] For a short perspective highlighting key methods for producing graphene monodispersions: A. A. Green, M. C. Hersam, *J. Phys. Chem. Lett.* **2010**, *1*, 544–549.
[68] C. Zhi, Y. Bando, C. Tang, H. Kuwahara, D. Golberg, *Adv. Mater.* **2009**, *21*, 2889–2893.
[69] a) Fluorescence quenching microscopy: J. Kim, L. J. Cote, F. Kim, J. Huang, *J. Am. Chem. Soc.* **2010**, *132*, 260–267; Gold coat: H. Zhou, C. Qiu, Z. Liu, H. Yang, L. Hu, J. Liu, H. Yang, C. Gu, L. Sun, *J. Am. Chem. Soc.* **2010**, *132*, 944–946.
[70] A method, not yet proven with graphene, creates one-molecule-thick organic nanosheets by self-assembly with CB[8] and dispersion by ultrasound: Q. An, Q. Chen, W. Zhu, Y. Li, C. Tao, H. Yang, Z. Li, L. Wan, H. Tian, G. Li, *Chem. Commun.* **2010**, *46*, 725–727.

Published online: April 1, 2010

